Multilayer-based radiation pulse slicers for Linac Coherent Light Source (LCLS) applications

Roman Tatchyn*
Stanford Synchrotron Radiation Laboratory, Stanford Linear Accelerator Center, Stanford, CA 94305, USA

ABSTRACT

The SLAC Linac Coherent Light Source (LCLS), an X-ray Free-Electron Laser (XRFEL) designed to operate over a fundamental energy range of 1 - 8.5 keV, is expected to produce ultra-short pulse lengths down to ~ 200 fs. Even though this represents an enormous decrease with respect to currently available high-brightness X-ray sources, it is believed that for a number of proposed LCLS applications (e.g., imaging or structural studies of molecular clusters with highly focused pulses) it will become necessary to reduce the pulse duration even further, possibly by as much as 1-2 orders of magnitude. Of the various compressive or chopping (i.e., slicing) optical techniques considered for shortening the pulse, the focus of one of our recent studies has been on a recently proposed slicing scheme based on the interaction of a longitudinally chirped LCLS pulse with a specially designed multilayer. The chopping mechanism is the selective reflection of only that sub-interval of the pulse that fulfills the multilayer Bragg condition. Of particular interest are the reflection efficiency and the distortion induced in the temporal fine structure of the reflected pulse, both of which can be critical to the efficacy of the scheme for a given application. Here we present results of selected parameter studies of different multilayer-based beam chopper systems using codes and LCLS radiation models developed at SSRL and LLNL.

Keywords: Free-Electron Laser (FEL), X-Ray Free-Electron Laser (XRFEL), Self-Amplified Spontaneous Emission (SASE), Linac Coherent Light Source (LCLS), temporal compression, time slicing, Fourier transform, multilayer, phase space, Bragg condition, impulse response, convolution

1. INTRODUCTION

In recent years, one of the more promising directions in Ångstrom-wavelength 4th Generation synchrotron radiation source development has been the linac-driven Free Electron Laser (FEL) operating in the Self-Amplified Spontaneous Emission (SASE) regime [1,2]. Fundamental characteristics of this source, when based on designs using present-day technology [3,4], include the attainment of fully transversely coherent output pulses with ~0.1% bandwidths, output powers of tens to hundreds of gigawatts, beam diameters of the order of 100 μm, beam divergences of the order of 1 μr, and output pulse lengths of the order of 100 femtoseconds. The advent of these parameters has in turn stimulated a widespread interest in the X-ray scientific community, and a number of workshops have been held in recent years to explore scientific applications made possible by this novel source [5,6,7,8]. One result of such assessments, presently being incorporated, for example, into the Conceptual Design Report of the SLAC Linac Coherent Light Source (LCLS) [9], has been the realization that a number of frontier scientific applications will require radiation phase space parameters of one-to-several orders of magnitude beyond those available in the raw FEL pulse [10,11]. As a consequence, directed efforts by the SLAC LCLS R&D Program's FEL Physics and X-Ray Optics groups have been undertaken to accomplish these goals [12]. One particularly challenging undertaking, the attainment of FEL pulse lengths down to the order of 10 fs using multilayers, is the subject of this paper.

*Corresponding author: Email: tatchyn@ssrl01.slac.stanford.edu; Telephone: 650-926-2731; FAX: 650-926-4100

2. LCLS TEMPORAL PULSE SLICING USING MULTILAYERS

The proposed slicing technique [13,14] is schematized in Fig. 1. An LCLS pulse with a longitudinal monotonic wavelength chirp $\Delta\lambda_{0N}(=\lambda_0 - \lambda_N)$ and total length L is made to intercept a multilayer with period d at an incidence angle θ. If some subinterval of the impinging pulse has a mean wavelength λ_i, which satisfies the multilayer Bragg condition $\lambda_i = 2d\sin\theta$, then that part of the subinterval that lies within the multilayer's passband, Δλ, will be reflected at an exit angle θ, while the remainder of the pulse will be scattered and absorbed.

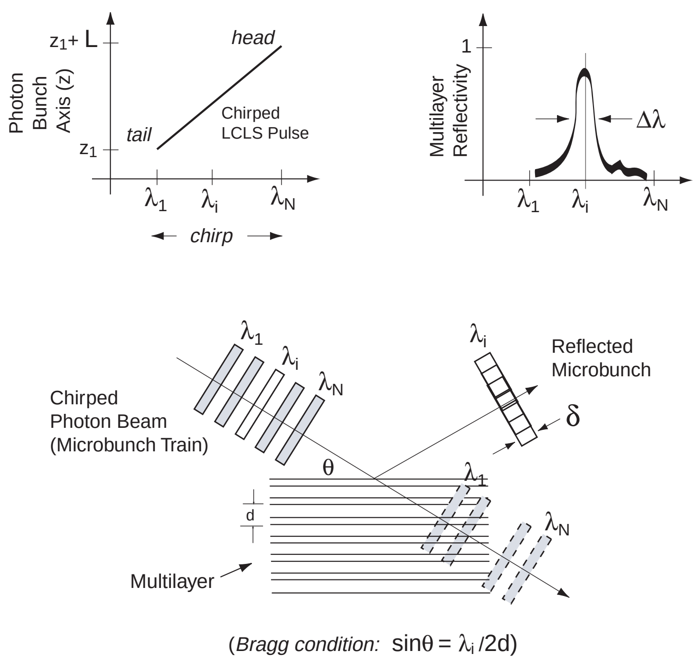

Figure 1. Wavelength dependence of chirped LCLS pulse (top left). Wavelength dependence of multilayer reflectivity (top right). Schematic side view of pulse/multilayer interaction (bottom).

If the impinging pulse is transversely coherent and its angular divergence is negligible (viz., λ<<D, where D is the pulse diameter), the longitudinal dimension of the reflected subinterval of mean wavelength λ_i can be expressed as

$$\delta = \frac{\Delta\lambda}{\Delta\lambda_{0N}} L + \delta' \quad .$$

(1)

Here the first term on the right represents a linear approximation to the length of the sliced pulse and δ" represents an additional minimal dilation stemming from the detailed time response of the multilayer to an incoming plane wave of finite longitudinal extent. In the following sections an analysis of a general multilayer's temporal response to radiation pulses of arbitrary temporal profile will be outlined and the results will be applied to practical multilayer systems interacting with LCLS radiation pulses.

3. MULTILAYER RESPONSE IN THE TEMPORAL DOMAIN

As has been shown elsewhere in the literature [e.g., 15,16,17], the response of a multilayer to a monochromatic plane wave of unit amplitude, frequency f, and incoming angle θ can be expressed as a complex reflectance, $\tilde{r}(f,\theta)=r(f,\theta)e^{i\phi_M(f,\theta)}$. More generally, if the incoming wave has the complex spectral-angular distribution $a(f,\theta)e^{i\phi_a(f,\theta)}$, then the reflected wave can be described by the complex amplitude $\tilde{a}(f,\theta)=a(f,\theta)e^{i\phi_a(f,\theta)}\tilde{r}(f,\theta)$. Following from general properties of linear systems [18], the temporal profile of the reflected wave is then given by the convolution of $\mathcal{F}^{-1}\{a(f,\theta)e^{i\phi_a(f,\theta)}\}$ with $\mathcal{F}^{-1}\{\tilde{r}(f,\theta)\}$, where the scripted F^{-1}s denote the inverse Fourier transforms of the quantities inside the curly brackets.

4. MULTILAYER NUMERICAL STUDIES

With reference to Eq. (1), it is evident that multilayers with the smallest bandwidths and highest reflectivities will yield the shortest pulse slices with the largest possible number of photons. To help identify candidate structures for LCLS pulse slicing applications a number of parameter studies of the W/B_4C system were first carried out for 1.5 Å radiation [12-14]. A code based on the rigorous dynamical matrix formalism of Abeles [15,19] was utilized for the calculations. The results, displayed in Fig. 2, indicate that reflectivities of ~60% and better can be attained with this system..

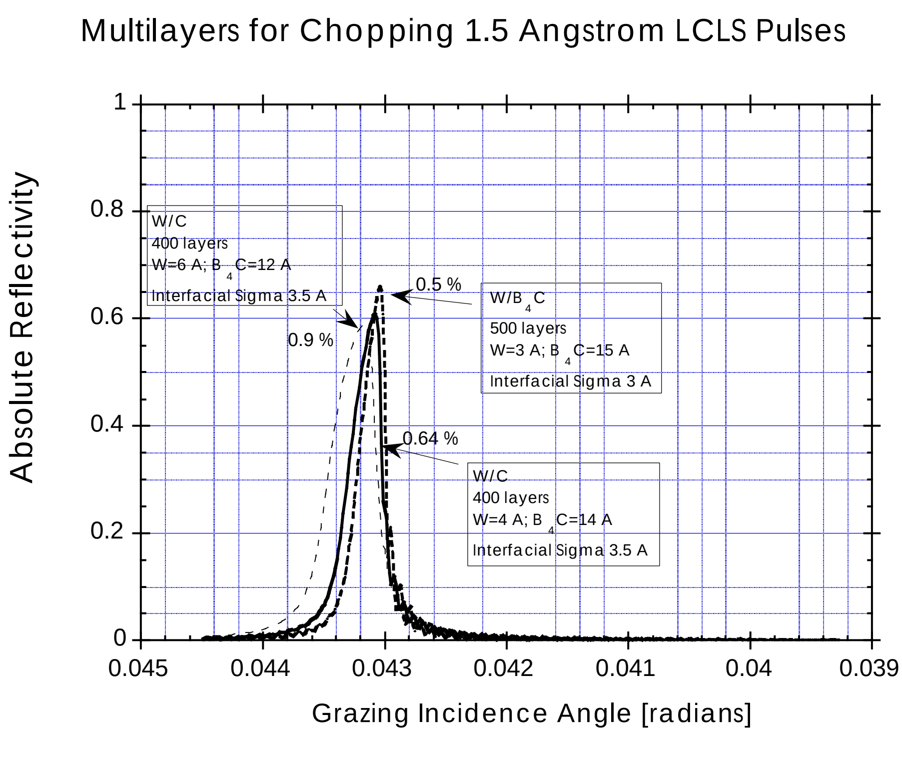

Figure 2. Reflectivity curves for W/B_4C multilayers with various parameter values adjusted for pulse slicing applications.

Next, the reflectivity of a Si/$MoSi_2$ system fabricated at LLNL [20] was calculated (see Fig. 3). This structure, featuring 1250 layer-pairs characterized by exceptionally small interfacial roughness of ~1 Å and a period of ~10 Å, features a reflectivity of ~ 56% and a bandwidth of ~ 0.17%, a factor of ~3 narrower than the smallest-bandwidth W/B_4C structure.

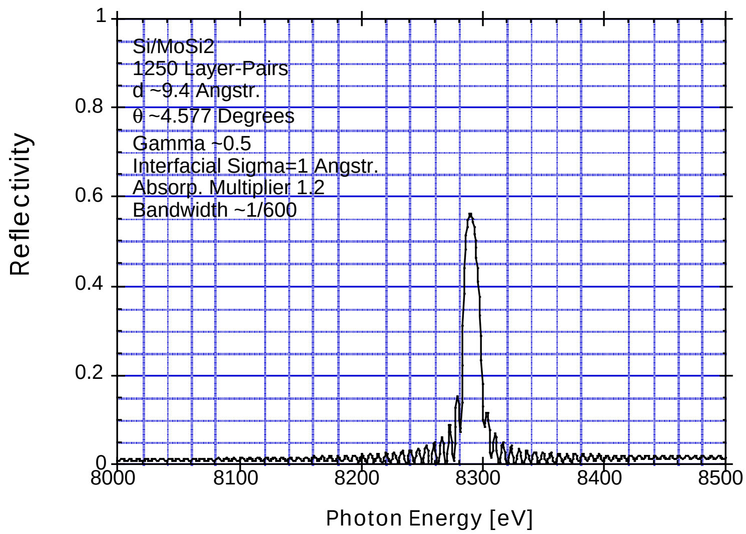

Figure 3. Reflectivity curve for Si/$MoSi_2$ multilayers fabricated at LLNL.

Next, the inverse Fourier transforms of the complex reflectance functions of the calculated multilayers were computed. The temporal response curve for Si/$MoSi_2$ is shown in Fig. 4, while the reflectivity of the smallest-bandwidth W/B_4C structure and the inverse Fourier transform of its complex reflectivity are shown in Figs. 5 and 6, respectively. The FWHM of the temporal response curves are seen to be consistent with the expected inverse scaling with respect to the FWHM multilayer bandwidths.

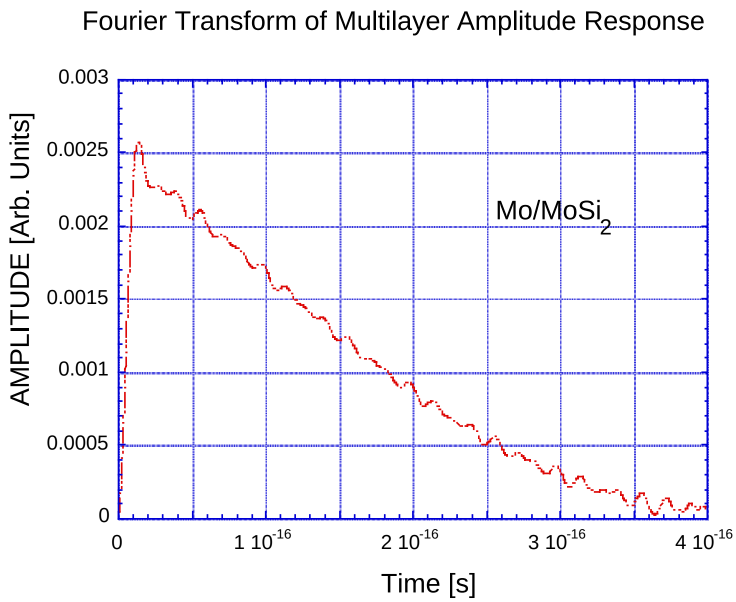

Figure 4. Temporal response curve of $Si/MoSi_2$ multilayer. The range of the abscissa corresponds to 800 wavelengths of 1.5 Å light.

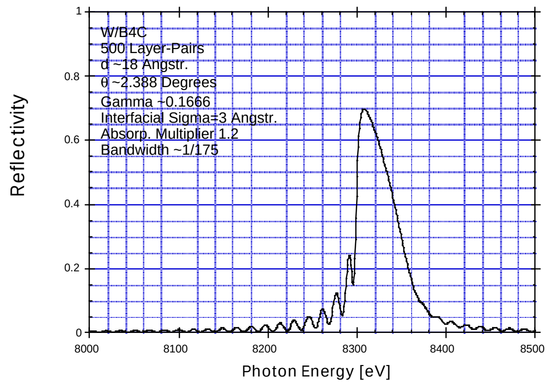

Figure 5. Reflectivity curve for W/B_4C multilayer.

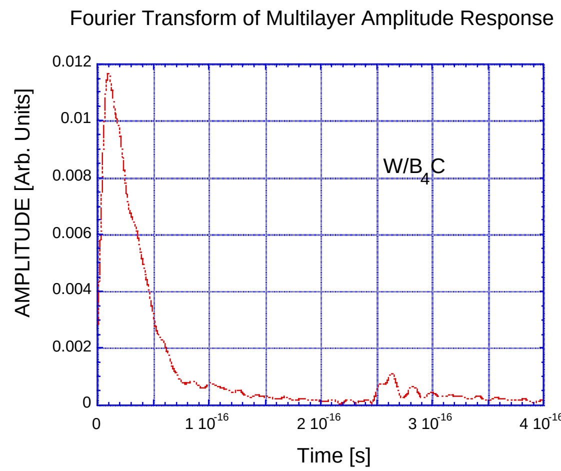

Figure 6. Temporal response curve of W/B_4C multilayer with an ~0.51% bandwidth. The second peak at ~2.6×10^{-16}s corresponds to a reflection of the incoming pulse off the multilayer substrate.

5. PULSE SLICING PERFORMANCE STUDIES

As discussed in detail elsewhere [21], an LCLS radiation pulse can be represented as a superposition of wavetrains randomly distributed in the longitudinal direction. For the purposes of this study we assume that a 1.5 Å LCLS pulse consists of ~1400 randomly distributed truncated sinusoids, each exactly 300 wavelengths long. To assess the response of a multilayer to the entire LCLS pulse the response of the multilayer to one of the truncated sinusoids comprising the pulse must first be calculated. Prior calculations [13-14] displaying the intensity profiles of an incoming and reflected 300-cycle sinusoidal pulse for the foregoing $Si/MoSi_2$ and W/B_4C structures are shown in Figs. 7 and 8. It is evident that the W/B_4C multilayer, with a substantially broader bandwidth and narrower temporal response, induces a substantially smaller amount of temporal distortion into the reflected pulse than the $Si/MoSi_2$ structure.

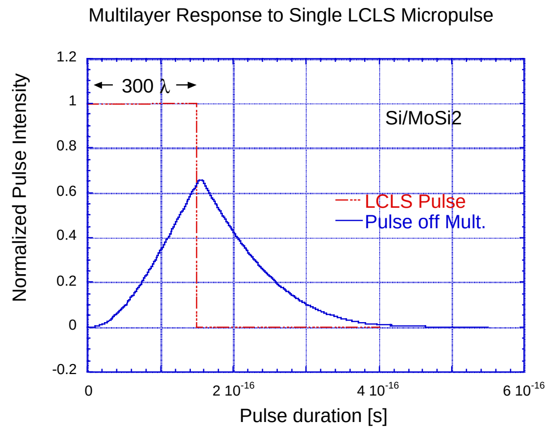

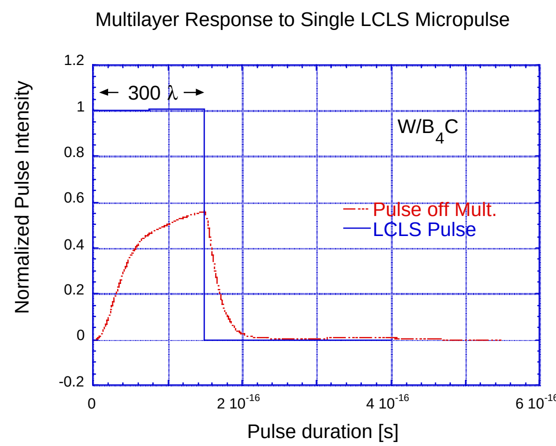

Figure 7. Temporal intensity profiles of an incoming truncated sinusoidal wave (rectangular pulse) and the

Figure 8. Temporal intensity profiles of an incoming truncated sinusoidal wave (rectangular pulse) and

same pulse reflecting off a $Si/MoSi_2$ multilayer.. the same pulse reflecting off a W/B_4C multilayer.

Finally, in order to illustrate the influence of the multilayers being studied on the temporal profile of the truncated pulse, we display 5 slippage lengths of the simulated LCLS pulse in Fig. 9 and the same pulse after reflecting off the $Si/MoSi_2$ multilayer in Fig. 10. It is evident that even for a multilayer with a relatively strong lengthening effect on the basic constituent wavetrain comprising the LCLS pulse the overall effect on the temporal profile is minimal·

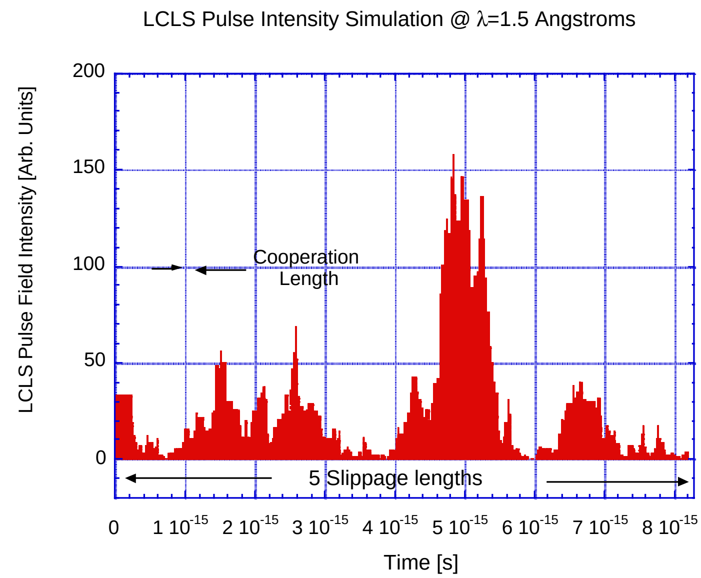

Figure 9. Temporal intensity profiles of a simulated LCLS pulse.

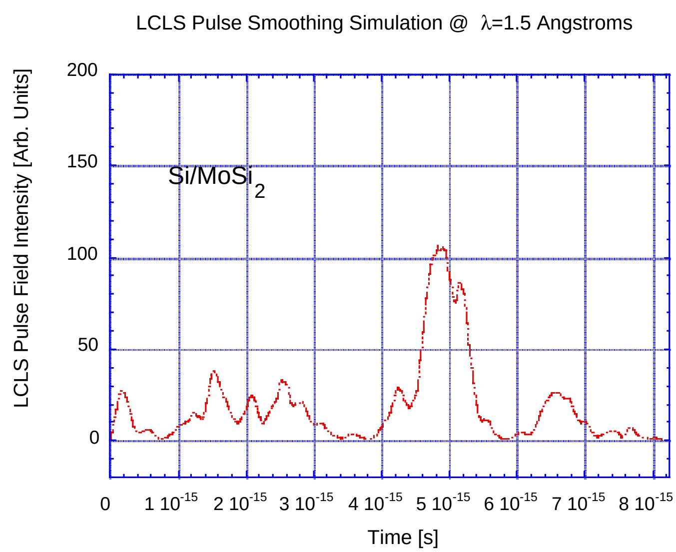

Figure 10. Temporal intensity profiles of a simulated LCLS pulse following reflection off a $Si/MoSi_2$ multilayer..

We can now consider the performance of specific multilayer pulse slicers for LCLS applications. In addition to the multilayers already computed we will also consider the fuller family of metal disilicide systems shown in Fig. 11 [20], which includes the Si/$MoSi_2$ reflectivity for comparison. We note that the narrowest bandwidth, ~0.09%, is predicted for the Si/$ZrSi_2$ system.

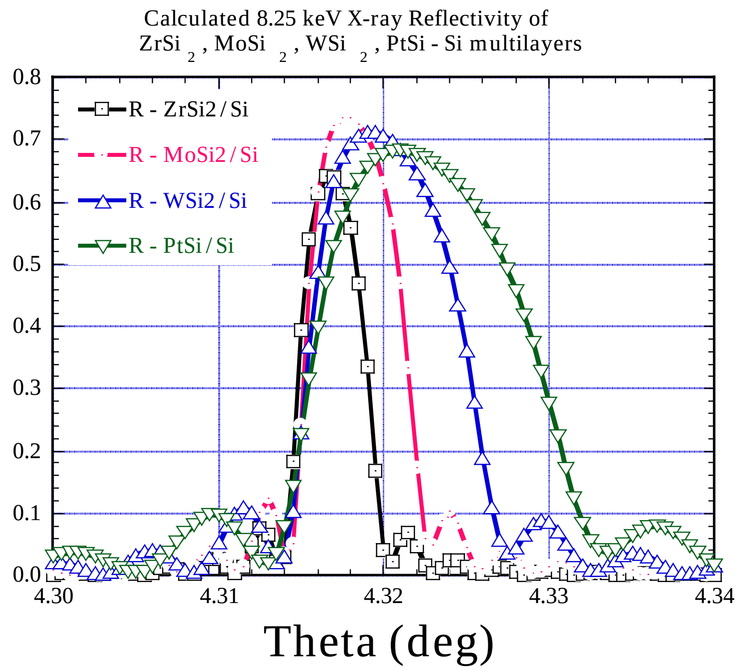

Figure 11. Reflectivity curves forn Si/metsal disilicide multilayers.

To calculate definite numbers, a set of four cases of electron beam compression and chirping is presented below in Table 1 [22]. We recall that for a given relative energy chirp in the electron beam, the photon beam from will exhibit a chirp approximately twice as large. Utilizing the preceding results, we can approximate the length of the sliced pulses for each of these cases with the first term in Eq. (1). For each of the four electron beam cases the results are tabulated for the W/B_4C, Si/$MoSi_2$, and Si/$ZrSi_2$ systems in Table 2. Clearly, when $\Delta\lambda > \Delta\lambda_{0N}$, no pulse length reduction is possible (Case 1).

Table 1.

Possible compression configurations to achieve 'short bunch'
April 17, 2000

compression scenario	e^- FWHM bunch length [fsec]	e^- FWHM energy spread [%]	Charge [nC]	CSR / wakefield 'risk'
Nominal	255	0.06	1	nominal
case-1	10	0.07	0.2	high
case-2	130	+0.20	1	high
case-3	670*	-0.25	1	low
case-4	255	+2.00	1	high

* peak current of just 1.5 kA requires emittance of ãå= 1 ìm

Table 2. Attainable sliced pulse lengths for the LCLS.

	BW [%]	Case 1	Case 2	Case 3	Case 4
W/B_4C	0.5	N/A	N/A	N/A	32 fs
$Si/MoSi_2$	0.17	N/A	~55 fs	~228 fs	~11 fs
$Si/ZrSi_2$	0.077	N/A	~25 fs	~103 fs	~5 fs

6. DISCUSSION

We have demonstrated that specially designed multilayers, when used to reflect LCLS 1.5 Å photon pulses with a lingitudinal wavelength chirp, are capable of slicing out subintervals of the pulse down to the sub-ten femtosecond range.

ACKNOWLEDGMENTS

Portions of his work were supported in part by the Department of Energy Offices of Basic Energy Sciences and High Energy and Nuclear Physics, and Department of Energy Contract DE–AC03–76SF00515. Other portions were supported by Department of Energy CRADA SLAC-9302.

REFERENCES

[1] J. B. Murphy, C. Pellegrini, "Introduction to the Physics of the Free Electron Laser," in *Frontiers of Particle Beams*, M. Month, S. Turner, eds., Lecture Notes in Physics No. 296, H. Araki et al, eds., Springer-Verlag, Berlin, 1988, pp. 163-212.

[2] K.-J. Kim, "Three Dimensional Analysis of Coherent Amplification and Self-Amplified Spontaneous Emission in Free-Electron Lasers," Phys. Rev. Lett. 57(13), 1871(1986).

[3] R. Brinkmann, G. Materlik, J. Rossbach, A. Wagner, eds., Conceptual Design of a 500 GeV e+e- Linear Collider with Integrated X-Ray Laser Facility, DESY 97-048, Hamburg, 1997.

[4] LCLS Design Study Group, Linac Coherent Light Source (LCLS) Design Study Report, SLAC-R-521, UC-414, 1998.

[5] J. Arthur, G. Materlik, H. Winick, eds., *Proceedings of the Workshop on Scientific Applications of Coherent X-Rays*, SLAC-437.

[6] B. H. Wiik et al, *International Workshop on "X-Ray Free Electron Laser Applications," (Copies of Transparencies),* Sept. 16-17, 1996, DESY, Hamburg, Germany.

[7] J. Arthur, I. Lindau, chairmen, *Workshop on the Science and Instrumentation for the Linac Coherent Light Source*, SLAC, Stanford, CA, USA, 15-16 October, 1999.

[8] C. Pellegrini, P. Chen, chairmen, SLAC Mini-Workshop on High Field, High Intensity Physics with the LCLS, SLAC, Stanford, CA, July 13, 2000, see http://www-ssrl.slac.stanford.edu/lcls/Workshops/.

[9] In progress, see http://www-ssrl.slac.stanford.edu/lcls/.

[10] R. Tatchyn, "LCLS Optics: Technological Issues and Scientific Opportunities," in *Proceedings of the Workshop on Scientific Applications of Short Wavelength Coherent Light Sources*, SLAC Report 414; SLAC-PUB 6064, March 1993.

[11] LCLS Scientific Advisory Committee, “LCLS: The First Experiments,” summary at http://www-ssrl.slac.stanford.edu/lcls/Workshops/ .

[12] V. Bharadwaj, A. Chao, M. Cornacchia, P. Emma, T. Kotseroglou, P. Krejcik, I. Lindau, H.-D. Nuhn, G. Stupakov, R. Tatchyn, R. Bionta, A. Toor, C. Pellegrini, "Ultrashort Optical Pulses in the Linac Coherent Light Source," (July 25, 2000), LCLS Technical Note 26) LCLS-TN-00-8.

[13] R. Tatchyn, proposed at the SRI'99 LCLS WorkshopRview/ Meeting, SSRL, 11/23/99; presented at the FEL Physics and X-Ray Optics R&D Groups Meeting on Short Pulses, LLNL, 12/17/99.

[14] Agenda Report, Third meeting of the LCLS Technical Advisory Committee at SLAC, May 19-20, 2000, see http://www-ssrl.slac.stanford.edu/lcls/papers/tac_071700.pdf.

[15] M. Born, E. Wolf, ***Principles of Optics***, Pergamon Press, London, 1975, Chapters 1

[16] H. A. MacLeod, *Thin-Film Optical Filters*, American Elsevier Publishing Company, Inc., New York, 1969.

[17] G. Fowles, *Introduction to Modern Optics*, Holt, Rinegart, and Winston, Inc., New York, 1975, Chapter 4.4.

[18] R. N. Bracewell, ***The Fourier Transform and its Applications***, 3rd ed. (Boston McGraw Hill, c2000).

[19] D. Boyers, A. Ho, Q. Li, M. Piestrup, M. Rice, R. Tatchyn, "Tests of variable-band multilayers designed for investigating optimal signal-to-noise versus artifact signal ratios in dual-energy digital subtraction angiography (DDSA) imaging systems,". Nucl Instrum Meth A346, 565(1994).

[20] T. Barbee, private communication.

[21] K.-J. Kim, "Temporal and Transverse Coherence of Self-Amplified Spontaneous Emission," LBNL-40672. June 1997.

[22] P. Emma, "Chirping the LCLS Electron Beam," (2000).LCLS-TN-00-6.